# COMPUTATION OF THE DENSITY DISTRIBUTION OF INJECTED NEUTRAL BEAM PARTICLES BY THE PROGRAM NEUDEN

F. P. Penningsfeld

IPP 4/229 November 1986

MAX-PLANCK-INSTITUT FÜR PLASMAPHYSIK

8046 GARCHING BEI MÜNCHEN

**MAX-PLANCK-INSTITUT FÜR PLASMAPHYSIK**

**GARCHING BEI MÜNCHEN**

# COMPUTATION OF THE DENSITY DISTRIBUTION OF INJECTED NEUTRAL BEAM PARTICLES BY THE PROGRAM NEUDEN

F. P. Penningsfeld

IPP 4/229 November 1986

*Die nachstehende Arbeit wurde im Rahmen des Vertrages zwischen dem Max-Planck-Institut für Plasmaphysik und der Europäischen Atomgemeinschaft über die Zusammenarbeit auf dem Gebiete der Plasmaphysik durchgeführt.*

## Errata

1. Equation (A-4) on page 14 should be read as

$$\sigma_{ii} = \rho Z^2 \left\{ \frac{1 - e^{-\beta v^2}}{v^2} - \beta \left(1 + \gamma v^2 - \delta v^2 e^{-\epsilon v^2}\right) e^{-\eta v^2} \right\}$$

2. The value of $\delta$ in expression (A-6) on page 14 is

$$\delta = \sqrt{M_b}\, 0.13893\ 10^{-7}$$

3. The correct version of equation (A-7) on page 15 is :

$$\sigma_{acx} = \rho v \left(1 + \beta v^3\ e^{-\gamma v}\right) e^{-\delta v}$$

# COMPUTATION OF THE DENSITY DISTRIBUTION OF INJECTED NEUTRAL BEAM PARTICLES BY THE PROGRAM *NEUDEN*

*F. P. Penningsfeld*

**Abstract**

The knowledge of the local density distribution of injected fast neutrals in a target plasma is necessary for the evaluation of most of the data sampled by the charge exchange recombination spectroscopy (CXRS) in combination with a diagnostic beam. This beam provides the population of fast neutrals exciting the spectral lines of the plasma particles observed by CXRS. The new computer program *NEUDEN* calculates this spatial distribution for each beam species separately along any arbitrary line of sight or even in a given plane of interest for survey purposes.

The program *NEUDEN* takes into account the actual beam parameters for $H^0$ or $D^0$ injection, i.e. the geometry of the injection box for up to six active sources, the shape of the extraction areas, divergence, power and energy of the beams, the ion species fractions and the corresponding neutralisation efficiencies. It also accounts for limiting apertures of arbitrary shape along the beam path. In this way the program is able to handle diagnostic beams as well as power injection systems.

The target plasma is regarded as a pure $H^+$, $D^+$ or $He^{++}$ plasma and is represented by the electron density $n_e(r)$, the mean temperatures $\bar{T}_e$ and $\bar{T}_i$ and an elliptical cross section with nested magnetic flux surfaces centered on the magnetic axis. The relevant cross sections for the beam attenuation by charge exchange and electron and ion collision processes with plasma particles for beam energy up to 120 keV $H^0$ (240 keV $D^0$ ) are reviewed and given in analytical formulas.

The influence of uncertainities in the input parameters on the results obtained by the program is estimated by a sensitivity study. This influence is found to be tolerable for the intended application. As an example the calculated density of the fast neutral particles in a helium discharge in the ASDEX tokamak is discussed.

## Table of contents

# I. INTRODUCTION

Charge exchange recombination spectroscopy (CXRS) may be used for the determination of the ion velocity distributions in magnetically confined plasmas /1/. By the observation of the profiles of spectral lines ion temperatures as well as bulk motions of plasma ion species can be measured containing informations about plasma rotation and impurity transport /2/. Furthermore the variations of the intensity of a chosen spectral line in space or time may be used to determine the local concentration of the corresponding plasma ion species as a function of time /3/.

The observed line radiation is emitted by excited, highly stripped, mostly hydrogenic ions which are generated by the interaction of the target plasma ion $A^{Z+}$ (e.g. $C^{6+}, O^{8+}, He^{2+}$) with an injected neutral beam $H^0(E)$ or $D^0(E)$ :

$$H^0(E) + A^{Z+} \quad \rightarrow \quad H^+(E) + A(n,l)^{(Z-1)+} \tag{1}$$

The excited atom of charge $Z-1$, described by the quantum numbers $(n,l)$ emits prompt line radiation in the frequency range from soft x-rays to the visible spectrum /4/ carrying informations about the motion of the particle in terms of Doppler broadening and Doppler shift of the observed spectral line.

The observation volume of such a CXRS diagnostic is defined by the intersection volume of the injected beam with the viewing cone of the spectrometer. In this way a well defined spatial resolution of the measurement can be achieved (see also Fig.1).

The intensity of a spectral line observed by the spectrometer with a sightline crossing the neutral beam due to prompt charge exchange recombination events is given by /1/

$$B_\lambda = \frac{1}{4\pi} \sum_{j=1}^{M} < \sigma v >_j^\lambda \int_L n_Z n_j dl \tag{2}$$

where $< \sigma v >_j^\lambda$ is the rate coefficent for the excitation of an atomic transition of wavelength $\lambda$ by the jth beam component. $n_Z$ denotes the local density of the

observed plasma ions and $n_j$ is the particle density of the beam species j. The integral is taken over the line of sight L of the spectrometer.

The excitation by slow beam halo neutrals as well as by the thermal neutral background can be neglected because the excitation rate coefficients decrease very fast for small relative velocities of the interacting particles (see for example /1/).

Assuming $n_Z = const$ in the observation region it becomes clear from equation (2) that the observed line intensity $B_\lambda$ depends on the line integrals of the particle densities $n_j, j = 1,2,3$ along the line of sight . In the case of a spatial scanning spectrometer optics the obtained signal is strongly affected by the absorption of the neutral beam in the target plasma. Therefore even for a relative determination of local impurity concentrations, the densities $n_j(\mathbf{x})$ of each neutral species must be known.

The computer program NEUDEN was written to perform the calculation of the densities $n_j(\mathbf{x})$ for a given injection geometry using a neutral beam model with single beamlet resolution and a simple plasma model , which may be extended for special applications.

## II. Principle of calculation

### II.1 The particle density of injected neutral atoms

The neutral beam is represented by a number $N_b$ of gaussian beamlets each delivering a particle flux density $i_j(\mathbf{x})$ of species j at the point of interest $A(\mathbf{x})$. To account for the absorption of the neutral beam penetrating into the target plasma the line integrated electron density

$$\int_0^A n_e db \tag{3}$$

between the center of each extraction hole and the point $A(\mathbf{x})$ is calculated . The corresponding local ion density is assumed to be $n_Z = n_e/Z_P$ where $Z_P$ denotes the charge of the plasma ions with density $n_Z$ . From the cross sections for electron and ion impact ionisation and charge exchange ionisation represented by analytical formulas ( see appendix ) the effective beam ionisation cross section $\sigma_{eff}(E_j, T_e)$ is computed .The transmission of each beamlet intensity from the edge of the plasma to the point $A(\mathbf{x})$ is then given by

$$i_b(x) = i_b(0)\; e^{-\sigma_{eff}\int_0^A n_e db} \tag{4}$$

where $i_b(0)$ denotes the incident intensity of the beamlet. The neutral density $n_j(\mathbf{x})$ of the species j at the point $A(\mathbf{x})$ is then given by the sum over all beamlet contributions divided by the particle velocity $v_j = v_0/\sqrt{j}$.

For survey purposes the points of interest are chosen in an arbitrary plane and the resulting densities are displayed in form of contour plots of each species (see e.g. Fig. 10 ). In case of a detailed analysis for a given line of sight the results $n_j(l)$ are plotted along this line of sight (e.g Fig. 11b ) and printed together with the line integrated neutral density for each species.

## II.2 Model of the neutral beam

The program **NEUDEN** includes the source geometry for up to 6 sources per beamline at different positions with individual beam steering and focussing . It computes from a given ion species mix the corresponding neutral power fractions taking into account the energy dependence of the neutralisation efficiency and the gas target density in the neutraliser. The effect of beam shaping apertures and of the duct entrance may be included by a polygonal approximation of the corresponding opening cross section given in form of a set of $N_A \leq 21$ points in 3D-coordinates. Each source generating a neutral beam of energy $E_0(keV)$ and power $P_N(kW)$ is divided into $N_b$ beamlets . The axis of each beamlet is defined by the position of its extraction hole and the focal point $F_i$ of the source $i$ (see also Fig. 3). A beamlet contributes only to the neutral density at the point $A(\mathbf{x})$ if its axis does not intersect the walls of the introduced apertures. The relevant parameters used for the beam model are listed in table I.

Table I : Beam parameters used in NEUDEN

| | |
|---|---|
| $P_n$ | neutral power per source in kW |
| $E_0$ | beam energy in keV |
| $N_b$ | number of beamlets per source |
| $f_{I_j}$ | normalized ion species fraction $j = 1, 2, 3$ |
| $\Theta_{1/e}$ | beamlet divergence (degree) |
| $\Pi_N$ | neutraliser target density $(cm^{-2})$ |
| $f_{i(h,v)}$ | horizontal resp. vertical focal length of the source i |
| $Q_i(x, y, z)$ | central point of the source i in beamline coordinates |
| $S_i(x, y, z)$ | aiming point of the source i in beamline coordinates |

The neutral power fractions $f_{N_j}$ are calculated from $\Pi_N$ and the given ion species mix using the neutralisation efficiency $\eta_N(E_j, \Pi_N)$ /6/ :

$$f_{N_j} = \frac{\eta_N f_{I_j}}{\sum_{j=1}^{3} \eta_N f_{I_j}} \tag{5}$$

with

$$\eta_N(E_j, \Pi_N) = \frac{\sigma_{10}}{\sigma_{01} + \sigma_{10}}(1 - e^{-(\sigma_{01}+\sigma_{10})\Pi_n}) \tag{6}$$

The particle flux density $i(z, \rho)$ in a plane vertical to the beamlet axis with distance $z$ to the extraction hole is assumed to be gaussian (see also Fig. 3) :

$$i(z, \rho) = \frac{i_{o,j}}{a^2}\, e^{-(\rho/a)^2} \tag{7}$$

$$a = z/tg\ \Theta_{1/e}$$

with the beamlet intensity given by

$$i_{o,j} = \frac{j\ f_{N_J}\ P_N}{N_b\ E_0} \tag{8}$$

## II.3 Model of the target plasma

The target plasma is regarded as a pure $H^+$ , $D^+$or $He^{++}$-plasma ( ion mass $A_P$ , ion charge $Z_P$ ) and it is represented by the electron density $n_e(r)$, the ion density $n_i(r) = n_e(r)/Z_P$ and the mean temperatures $\bar{T}_e$ and $\bar{T}_i$. The plasma cross section is assumed to be elliptical ( half axes a, b ) with flux surfaces nested on a circular magnetic axis. For the calculation of the line integrated plasma density each point along the path of integration is transformed into the poloidal coordinate system to obtain the effective minor radius $\xi = \xi(r, \theta)$ defining the local density by

$$n_e(\xi) = n_0(1 - \xi^\alpha)^\beta \tag{9}$$

The exponents $\alpha$ and $\beta$ may be chosen to fit a measured density profile with peak density $n_0$ (see also Fig. 4).

## II.4 Description of the geometry

The whole calculation and the representation of the results is performed in the beamline coordinate system (Fig. 1). The relative position of the target plasma is given by the toroidal coordinates of the Pivot point $P(R_P, \Phi_P, z_P)$, the injection angle $\phi_I$ and the distance $PO$. These input parameters provide the information for the transformations from the beamline to the plasma coordinate system to get the local plasma density for the calculation of the beam absorption.

The chosen line of sight has to be given by the beamline coordinates of the two end points $C$ and $D$ (see Fig. 11b for example). In the case of a contour plot the observation plane has to be defined by three edge points $E_1, E_2, E_3$.

## III. Sensitivity study

The computed density of fast neutrals is influenced by a lot of parameters used in the models for beam and plasma . These parameters are not always well known due to incomplete beam diagnostics or experimental errors of the corresponding measurements. A sensitivity study was performed to estimate the influence of the most important parameters on the obtained results for the neutral densities along a given line of sight. For this purpose the same geometry as used in section IV was assumed, with the exception that only one source centered on the beamline axis is active. This simplifies the interpretation of the effects.

As a figure of merit the relative variation of the peak density

$$\frac{\Delta n_{j,max}}{n_{j,max}} \tag{10}$$

and the relative variation of the line integrated neutral density along the path $C \rightarrow D$ of the CXRS diagnostic (see also Fig 11a)

$$\frac{\Delta \int_C^D n_j(l)dl}{\int_C^D n_j(l)dl} \tag{11}$$

are calculated for some characteristic parameter variations. The values of the two figures of merit according equations (10) resp. (11) differ only remarkably if the corresponding parameter causes a change of the beam profile. Therefore only for the parameter $\Theta_{1/e}$ both values are plotted. For all runs of the sensitivity study the neutral power $P_N$ of the beam is kept constant.

It shows up that the results of the code NEUDEN depend very sensitively on the assumed species mix for a fixed transmitted beam power (Fig. 4a,b,c). Moreover the variation of the input ion species mix changes not only the particle density of the beam components but also their penetration behaviour. This in turn implies a spatially varying deviation of the obtained results for erroneous input data.

A strong influence on the variation of the peak neutral density is also found for the beamlet divergence (Fig. 5a). But the deviation of the line integrated values

which are more relevant for the CXRS diagnostic show only a more or less linear dependence on $\Theta_{1/e}$ (Fig. 5b). The relative variations of the code results due to variations in $E_b$, $\Pi$ and $\bar{T}_e$ are all found to stay below 6 to 7% in the assumed parameter range. The influence of slightly different ( e.g. time varying ) density profiles as shown in Fig.9 is also not very pronounced and stays below 7% in this example.

Table II

| *parameter varied* | *standard case* | *see Fig.* |
|---|---|---|
| ion species mix | 50 : 30 : 20 | 4 a, b, c |
| beamlet divergence | $1.2^0$ | 5 a, b |
| beam energy | 40 (keV) | 6 |
| neutraliser target | $10^{16}\ cm^{-2}$ | 7 |
| plasma electron temperature | 1.5 (keV) | 8 |

Although the code is not able to handle target plasmas with a minority or impurity ion species, the effect of the presence of a minority ion species with charge $Z_M$ may be estimated by the interpolation between the results obtained for a pure $He^{++}$ and a pure $H^+$ run. Thereby it is assumed that the beam absorption by ionisation due to plasma ions ($n_i(r)$) and minority ions ($n_M(r)$) depends linearly on the ion densities in the range

$$0 \leq \alpha = \frac{n_M}{n_i} \leq 1 \tag{12}$$

For a given concentration $\alpha$ of minority ions ( here $H^+$ ) the relative deviation of the code results from the case of a pure $He^{++}$ plasma can be estimated according

$$\frac{\Delta n_j}{n_j} = \alpha \left( \frac{Z_p}{Z_M} - 1 \right) \frac{\Delta n_j}{n_j}\bigg|_{\alpha=1} \tag{13}$$

The variation between a pure $H^+$-plasma ( $\alpha = 1$) and a pure $He^{++}$-discharge ($\alpha = 0$) is found to be -1% for the $E_0$ component and -20% resp. -23% for the half and one third energy components. Therefore it may be concluded that the effect of the presence of minority ions for concentrations $\alpha \leq 0.10$ is also negligable.

## IV. Application to ASDEX discharges

As an example for the application of NEUDEN the density of fast neutrals in front of the SO injector of ASDEX is calculated for two shot series. In both cases a hydrogen beam beam was injected into a NI heated Helium discharge . The target plasma can be described at the time $t \approx 1.5\ s$ by the parameters (see also Fig. 9)

$$(14) \qquad n_e(0) = 4.1\ 10^{13}\ , \quad \alpha = 2.0\ , \quad \beta = 0.75\ , \quad \bar{T}_e = 1.8\ (keV)$$

In the shots 17915-17 only the upper two of the four sources of the SO injector were operated at an extraction voltage of 41 (keV) delivering the power of 870 (kW) into the torus. Fig. 11a shows the resulting neutral density along the beamline axis . In Fig. 11b the neutral density for each species along the line of sight of the CXRS diagnostic in the $z = 0$ plane is plotted . The density distribution produced by these sources is not symmetric to the midplane ($z = 0$) because the two beam axes of the sources intersect the diagnostic plane at $z_b = 1.9$ cm. The values of the line integrated density of fast neutrals along the CXRS axis for each beam species are also given for this example.

The shots 17918-25 were performed with the two lower sources of the injector box tuned to 25 keV delivering 320 kW of neutral power. Figures 12a and 12b show the corresponding results.

For the treatment of a shot with different beam energies one separate run of NEUDEN is needed for each energy value. The total density of fast neutrals at a given point or the total line integrated density are obtained by summing up the results for the three different species of each injection energy . Although this sum gives the total density of fast neutrals at a fixed point, it should be mentioned that this value is not very useful for the evaluation of the CXRS data because of the strong dependence of the excitation cross sections on the velocity of the incident particles due to the implicit assumption $v_b > v_{therm}$.

## V. Conclusions

The new program **NEUDEN** described in this report is able to calculate the density of fast injected neutral atoms in a reliable way for a wide variety of injection geometries and beam parameters. By means of a sensitivity study a strong influence of the assumptions about species mix and beamlet divergence on the code results is found.

The experimental errors of other parameters, e.g. beam power, beam energy, neutralisation efficiency, gas target thickness or plasma electron temperature and density profile do not affect the code results strongly. Even the existence of a minority ion species should be tolerable up to concentrations of $\alpha \approx 10$ to 15% .

From these results one concludes that the program **NEUDEN** is a suitable tool for the data evaluation of an active CXRS diagnostic. If the input parameters of species mix and beamlet divergence are carefully checked, an accuracy of the code results of better than 20 % is possible. But this implies that specific runs of the program are necessary for each shot series.

In the case of a large observation volume of the CXRS-diagnostic a weighting procedure for different lines of sight inside the total viewing cone should be used to get the correct value for the effective line integrated neutral density which contributes to the total line intensity detected by the spectrometer.

## Appendix

### Analytical expressions used for the cross sections of beam attenuation

The cross sections for beam attenuation by charge exchange and electron and ion impact ionisation in the target plasma are represented by analytical expressions given by Galbraith and Kammash /5/. These formulas are integrable analytically over the velocity distribution of the target particles and therefore it becomes easier to account for finite ion temperatures if the usual approximation $v_b >> v_{thermal\ ion}$ does not hold anymore.

### beam ionisation by electron impact

The ionisation rate of a neutral beam (energy $E_b$(keV), mass $M_b$(amu) ) by a maxwellian electron distribution of temperature $T_e$ given in ref /5/ in the approximation $v_b << v_e$ is :

$$(A\text{-}1) \qquad < \sigma v > \; = \; 2\rho\sqrt{\alpha}\,\{\frac{1-\beta}{\sqrt{\pi}} + \beta\, u\, e^{u^2}(1-\Phi(u))\}$$

with $\Phi(u)$ denoting the error function of the argument u . The values for $\sigma_{ie}$ as plotted in Fig 2a,b are obtained using following parameters ($T_e = 1kev$) :

$$\alpha = \frac{2.843}{T_e}\ 10^{-19}, \qquad \beta = 0.581,$$

$$(A\text{-}2) \qquad \gamma = 0.1875\ 10^{-9}, \qquad \rho = 70.21, \qquad u = \frac{\gamma}{2\sqrt{\alpha}}$$

The plotted cross sections as a function of beam energy are obtained by dividing the reaction rate by the beam velocity

$$(A\text{-}3) \qquad v_b \; = \; 4.376\ 10^7 \sqrt{\frac{E_b}{M_b}}$$

**beam ionisation by ion impact**

The ion impact ionisation in the present version of *NEUDEN* is calculated in the approximation $v_b >> v_{thermal\ ion}$ :

$$\sigma_{ii} = \rho Z^2 \{\frac{1 - e^{\beta v^2}}{v^2} - \beta\left(1 - \gamma v^2 - \delta v^2 e^{-\epsilon v^2}\right) e^{-\eta v^2}\} \qquad \text{(A-4)}$$

$v \approx v_b$ denotes the relative velocity of the interacting particles . In table III the parameter sets for equation A-4 are given for the the different plasma species considered. In case of the hydrogen plasma the fit recommended by Rudd et al./9/ is reproduced very well. The parameters for the $He^{++}$ case are chosen by the author to fit the experimental data given by Shah and Gilbody /8/ for the ionisation of atomic hydrogen by fast $He^{++}$ ions.

| Parameter | $H^+$ plasma (resp. $D^+$) | $He^{++}$ plasma |
|---|---|---|
| $\rho$ | 36.723 | 25.900 |
| $\beta$ | $0.00654\ 10^{-15}$ | $0.00654\ 10^{-15}$ |
| $\gamma$ | $0.06474\ 10^{-15}$ | $0.07580\ 10^{-15}$ |
| $\delta$ | $0.00285\ 10^{-15}$ | $0.00285\ 10^{-15}$ |
| $\epsilon$ | $0.67235\ 10^{-15}$ | $0.67235\ 10^{-15}$ |
| $\eta$ | $0.06515\ 10^{-15}$ | $0.04170\ 10^{-15}$ |

**charge exchange ionisation of the neutral beam**

Following Galbraith and Kammash /5/ the cross section for the CX reactions between hydrogen isotopes may be fitted by :

$$\sigma_{cx} = \rho\left(1 + \beta\ v^4\ e^{-\gamma v^2}\right)\ e^{-\delta v} \qquad \text{(A-5)}$$

with v denoting the relative velocity of the particles and

$$\rho = 3.644.\ 10^{-15}, \quad \beta = M_b^2\ 4.82\ 10^{-33}$$

$$\gamma = M_b\ 0.03655\ 10^{-15}, \quad \delta = \sqrt{M_b}\ 0.3893\ 10^{-7} \qquad \text{(A-6)}$$

The results obtained by this analytic representation compare very well with the data compiled in the report IPPJ-AM-30 /10/.

The fit for CX reactions of a $He^{++}$ projectile with a hydrogen target are also given in reference /5/ in terms of the relative particle velocity :

(A-7) $$\sigma_{acx} = \rho v \left(1 + \rho v^3 \, e^{-\gamma v}\right) e^{-\delta v}$$

with the parameters

$$\alpha = M_{He} \; 0.5221 \; 10^{-15}, \quad \beta = 0.3 \; \alpha^{1.5}$$

(A-8) $$\gamma = 0.4\sqrt{\alpha}, \quad \delta = 0.258 \; \sqrt{\alpha}, \quad \rho = 1.756 \; 10^{-16} \; \sqrt{\alpha}$$

$M_{He}$ denotes the $He^{++}$ mass in amu. A comparison of $\sigma_{acx}$ calculated by equation (A-7) shows a very good agreement with the experimental data compiled in reference /10/ in the energy range from 1 to 200 (kev/amu).

**the effective cross section for beam attenuation used in *NEUDEN***

The line integral needed for the calculation of the beamlet transmission to a given point **A**

$$\int_0^A (\sigma_{ii} \; n_z + \sigma_{cx} \; n_z + \sigma_{ie} \; n_e) db$$

is approximated by the product of the effective cross section $\sigma_{eff}$ and the line integrated electron density according :

(A-9) $$\sigma_{eff} \int_0^A n_e \; db \;\; = \;\; \left(\frac{\sigma_{ii} + \sigma_{cx}}{Z_p} + \sigma_{ie}\right) \int_0^A n_e \; db$$

Thereby an ion density $n_z = n_e / Z_p$ (see also equ.(4) )is assumed and the effects of a temperature profile $T = T(r)$ on the cross sections are neglected.

## References


1. R.J. Fonck, D.S. Darrow, K.P. Jaehnig, Phys. Rev. A **29** (1984), p. 3288.

2. K.P. Jaehnig ,R.J. Fonck , K. Ida, E.T. Powell, Rev. Sci. Instr. **56** (1985), p. 865.

3. M. v. Hellermann, *An active neutral beam diagnostic system for JET*, "JET report", 1985.

4. R. C. Isler, Phys. Rev. Lettr. **38** (1977), p. 1359.

5. D.L. Galbraith, T. Kammash, *Analytical approximations to the rate coefficients for charge exchange and ionization of neutral beams*, Nucl. Fus. **19(8)** (1979), p. 1047.

6. J. Kim , H. H. Haselton, J. Appl. Phys. **50(6)** (1979), p. 3802.

7. A.C. Riviere, Nucl. Fus. **11** (1971), p. 363.

8. M.B. Shah , H.B. Gilbody, J. Phys. B : At. Mol. Phys. **14** (1981), p. 2361.

9. M.E. Rudd, Y.-K. Kim, D.H. Madison, J.W. Gallagher, *electron production in proton collisions : total cross sections*, Rev. Mod. Phys. **57(4)** (1985).

10. H. Tawaka , T. Kato , Y. Nakai, *Cross sections of charge exchange transfers of highly ionized ions in hydrogen atoms*, "report IPPJ-AM-30", 1984.

## Figure captions

Fig. 1 : schematic view of the active CXRS-diagnostic system with the used coordinates and geometric parameters

Fig. 2a : cross sections for the ionisation of a hydrogen or deuterium beam in a hydrogen or deuterium target plasma

Fig. 2b : cross sections for the ionisation of a hydrogen or deuterium beam in a helium target plasma

Fig. 3 : illustration of the beamlet model used in NEUDEN

Fig. 4a,b,c: relative variation of the peak density for the three velocity components of fast neutrals with increasing $f_{I1}$ (full energy ion species) at fixed neutral power $P_N$ . The half energy component $f_{I2}$ is concerned as a parameter thereby fixing the $E_0/3$ species fraction by the normalisation.

Fig. 5a : variation of the peak neutral density with the beamlet divergence $\Theta_{1/e}$ according equ. (10)

Fig. 5b : variation of the line integrated density with the beamlet divergence $\Theta_{1/e}$ according equ. (11)

Fig. 6 : variation of the peak neutral density with the beam energy

Fig. 7 : variation of the peak neutral density with the neutralizer gas target density $\Pi$

Fig. 8 : variation of the peak neutral density with the electron temperature $T_e$ of the target plasma

Fig. 9 : measured electron density in ASDEX fitted by eq.(9) using 5 different parameter sets . The density profiles labeled $1 \rightarrow 4$ are used for the sensitivity study

Fig. 10a,b,c : example of the contour plot facility of NEUDEN for the three beam species of the lower two sources of the ASDEX SO injector operated at 25 keV

Fig. 11a : density of fast neutrals $n_j(\mathbf{x})$ for the three beam species of the upper two sources of the SO beamline operated at 41 keV calculated along the beamline axis

Fig. 11b : same as fig 6a, calculated along the CXRS line of sight denoted by the points $C$ and $D$ in fig 10a.

Fig. 12a : same as fig 12a for the lower sources operated at 25 keV

Fig. 12b : same as fig 12b for the lower sources operated at 25 keV

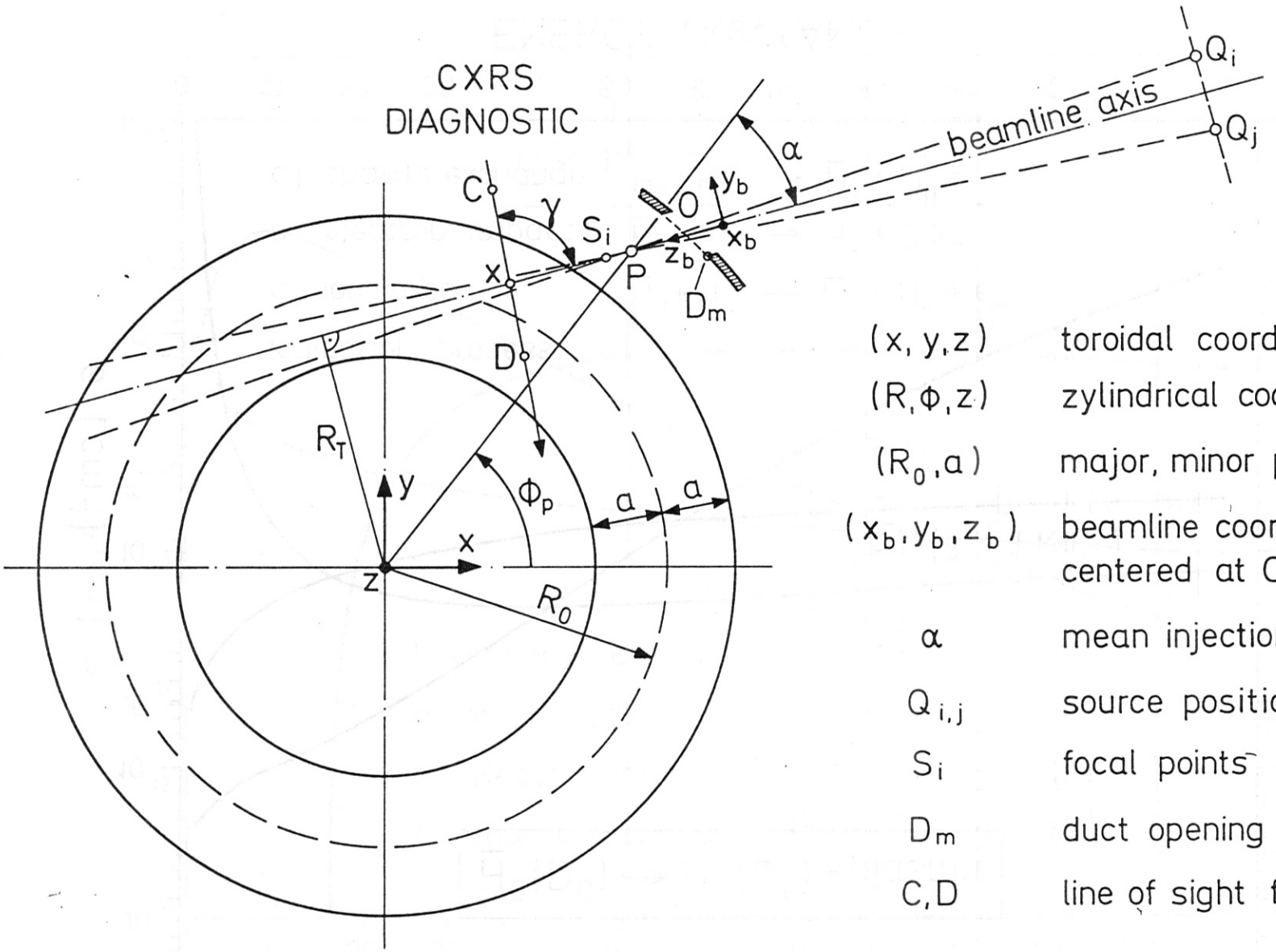


| | |
|---|---|
| $(x, y, z)$ | toroidal coordinates |
| $(R, \phi, z)$ | zylindrical coordinates |
| $(R_0, a)$ | major, minor plasma radius |
| $(x_b, y_b, z_b)$ | beamline coordinates centered at O |
| $\alpha$ | mean injection angle |
| $Q_{i,j}$ | source positions ( $i, j \leq 6$ ) |
| $S_i$ | focal points |
| $D_m$ | duct opening ( $m \leq 21$ ) |
| C, D | line of sight for CXRS |

*Fig. 1*

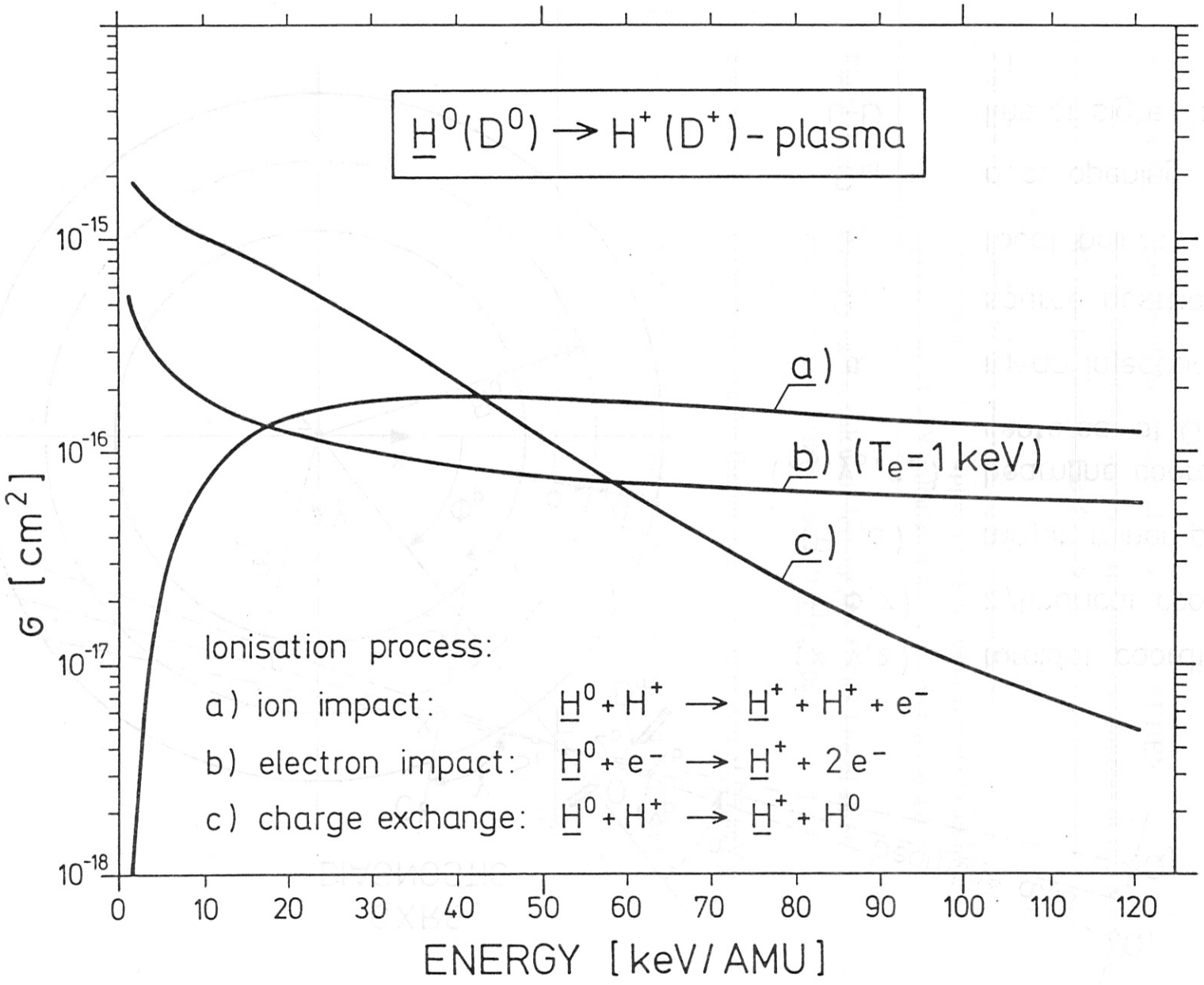
H⁰(D⁰) → H⁺(D⁺) - plasma
σ [cm²]
10⁻¹⁵
10⁻¹⁶
10⁻¹⁷
10⁻¹⁸
a)
b) (Tₑ=1 keV)
c)
Ionisation process:
a) ion impact: H⁰ + H⁺ → H⁺ + H⁺ + e⁻
b) electron impact: H⁰ + e⁻ → H⁺ + 2 e⁻
c) charge exchange: H⁰ + H⁺ → H⁺ + H⁰
0 10 20 30 40 50 60 70 80 90 100 110 120
ENERGY [keV/AMU]

*Fig. 2a*

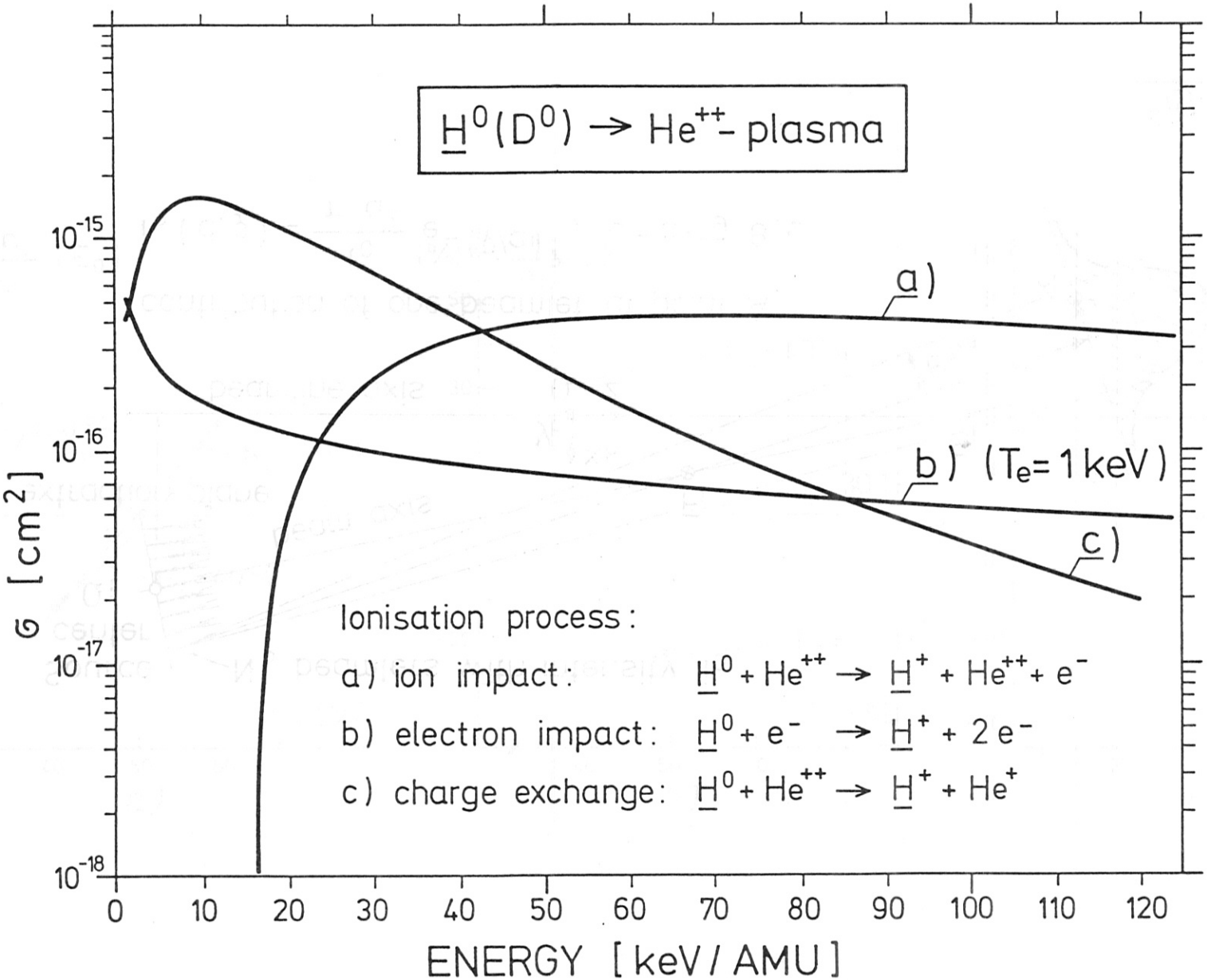
H⁰(D⁰) → He⁺⁺- plasma
a)
b) (Te= 1 keV)
c)
Ionisation process:
a) ion impact: H⁰ + He⁺⁺ → H⁺ + He⁺⁺ + e⁻
b) electron impact: H⁰ + e⁻ → H⁺ + 2 e⁻
c) charge exchange: H⁰ + He⁺⁺ → H⁺ + He⁺
σ [cm²]
10⁻¹⁵
10⁻¹⁶
10⁻¹⁷
10⁻¹⁸
0
10
20
30
40
50
60
70
80
90
100
110
120
ENERGY [keV / AMU]

Fig. 2b

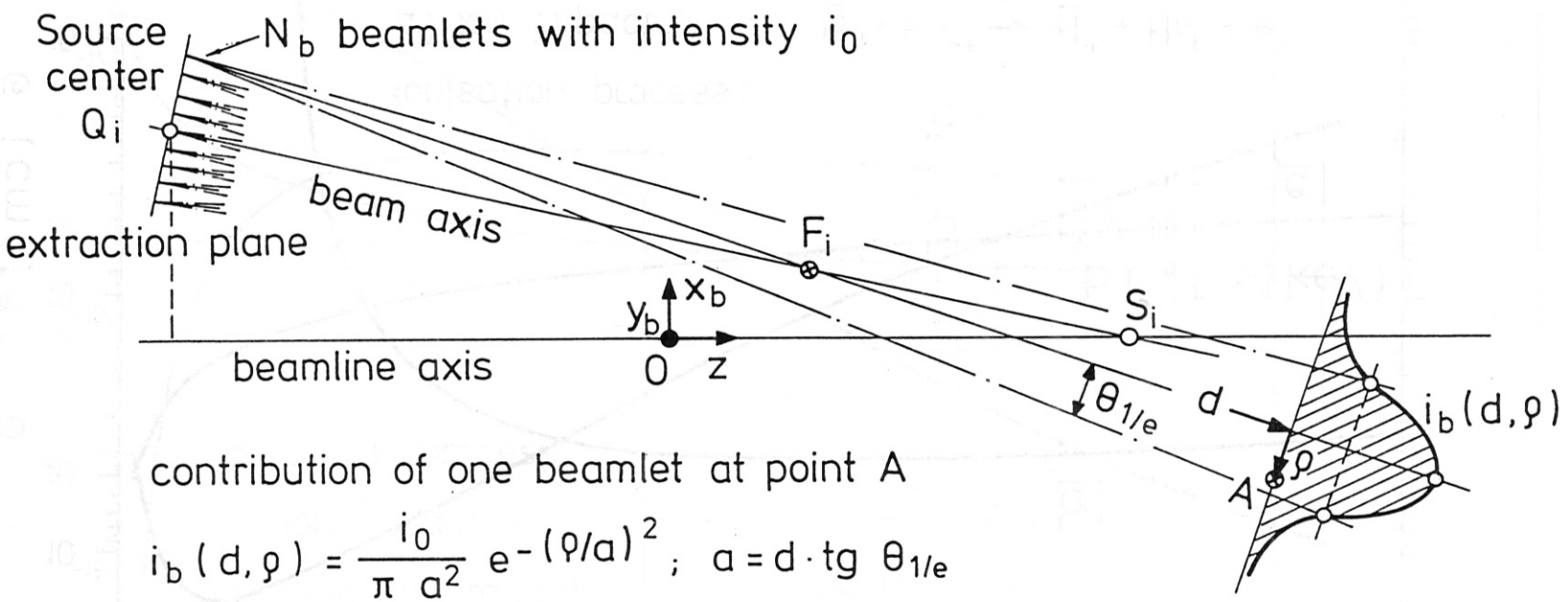


contribution of one beamlet at point A

$$i_b(d,\rho) = \frac{i_0}{\pi\, a^2}\, e^{-(\rho/a)^2}\,;\quad a = d \cdot \mathrm{tg}\ \theta_{1/e}$$

*Fig. 3*

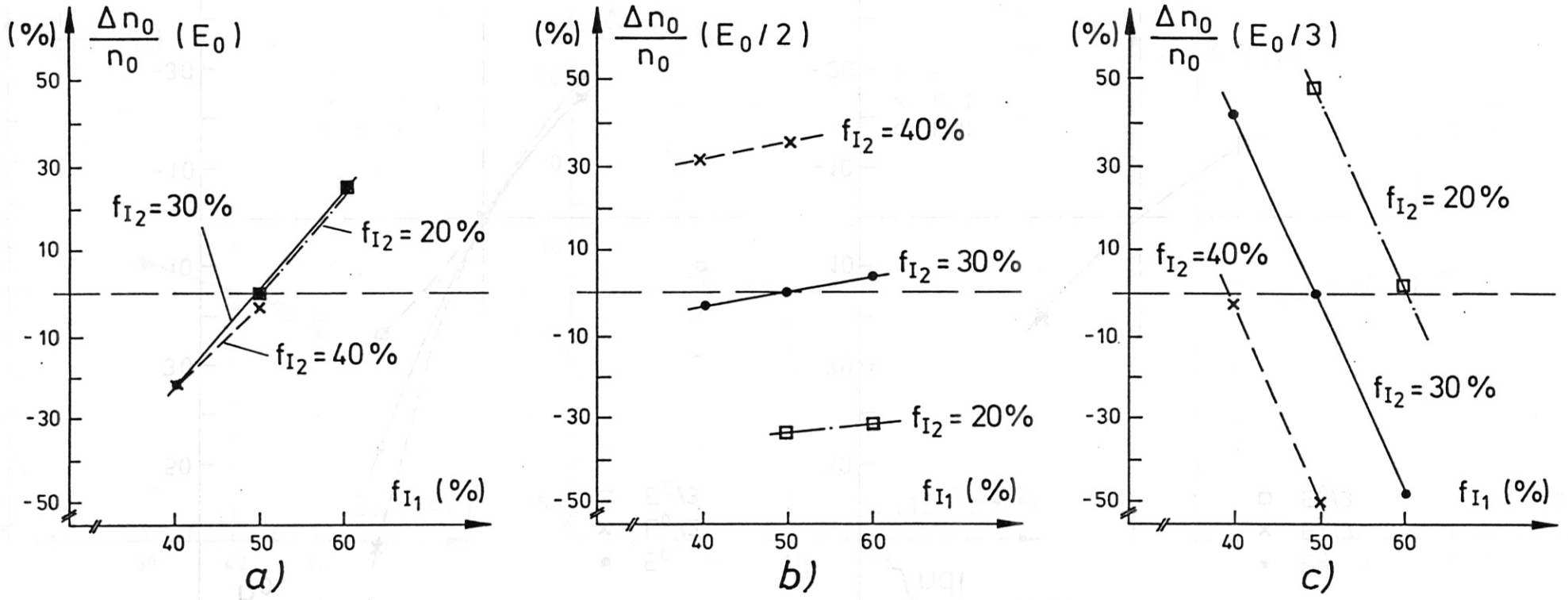
(%)
Δn0/n0 (E0)
50
30
10
-10
-30
-50
fI2=30%
fI2 = 20%
fI2 = 40%
fI1 (%)
40
50
60
a)
(%)
Δn0/n0 (E0/2)
fI2 = 40%
fI2 = 30%
fI2 = 20%
b)
(%)
Δn0/n0 (E0/3)
fI2 = 20%
fI2=40%
fI2 = 30%
c)

Fig. 4

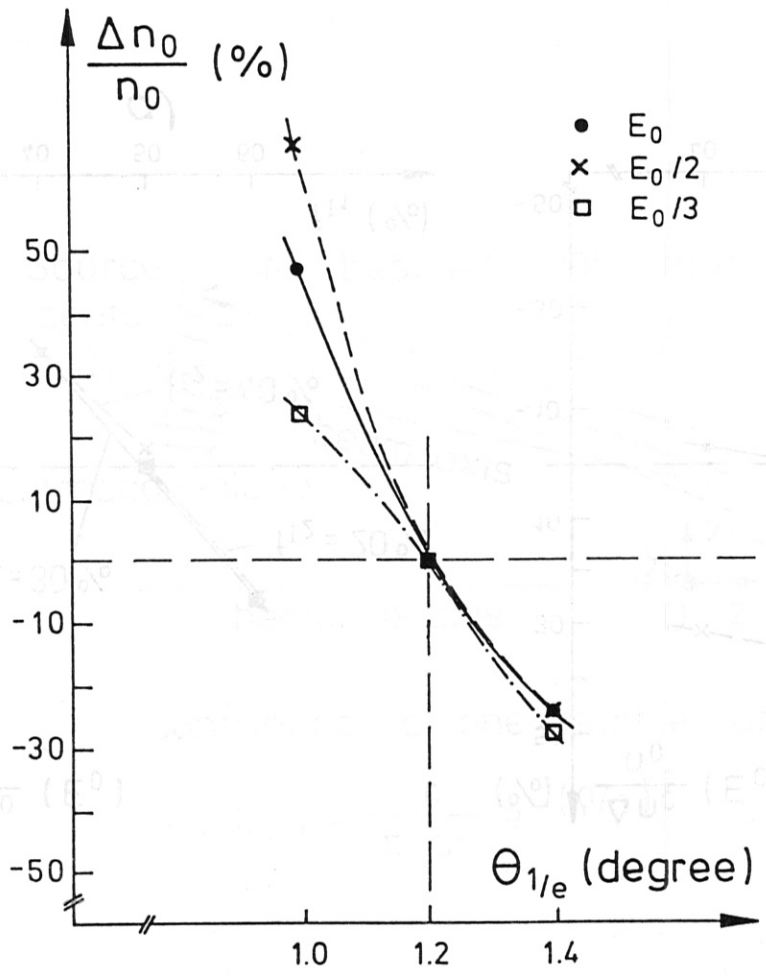
Δn0/n0 (%)
E0
E0/2
E0/3
50
30
10
-10
-30
-50
θ1/e (degree)
1.0
1.2
1.4

Fig. 5a

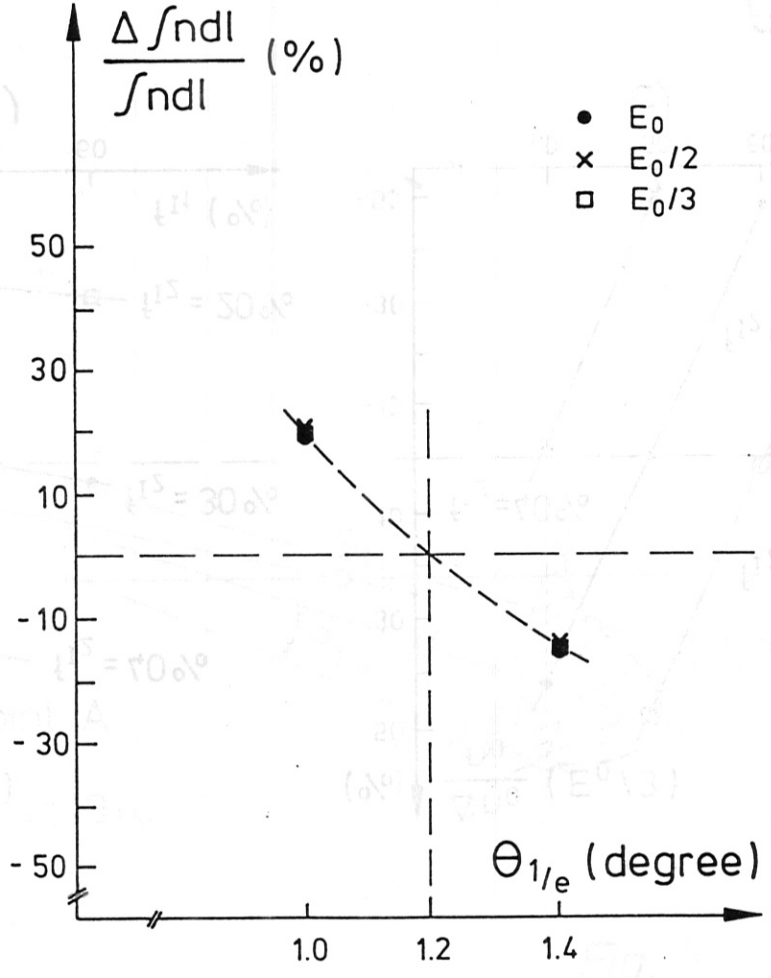
Δ∫ndl/∫ndl (%)
E0
E0/2
E0/3
50
30
10
-10
-30
-50
θ1/e (degree)
1.0
1.2
1.4

Fig. 5b

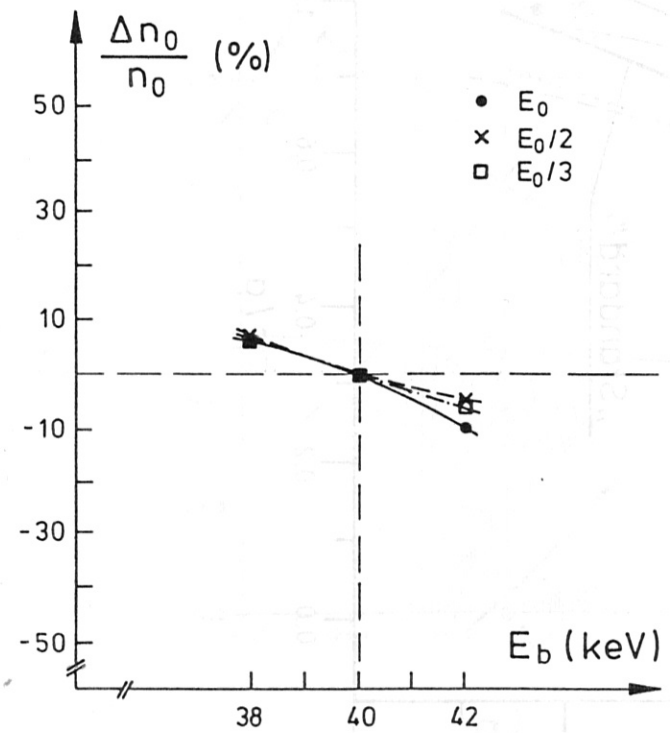


Fig. 6

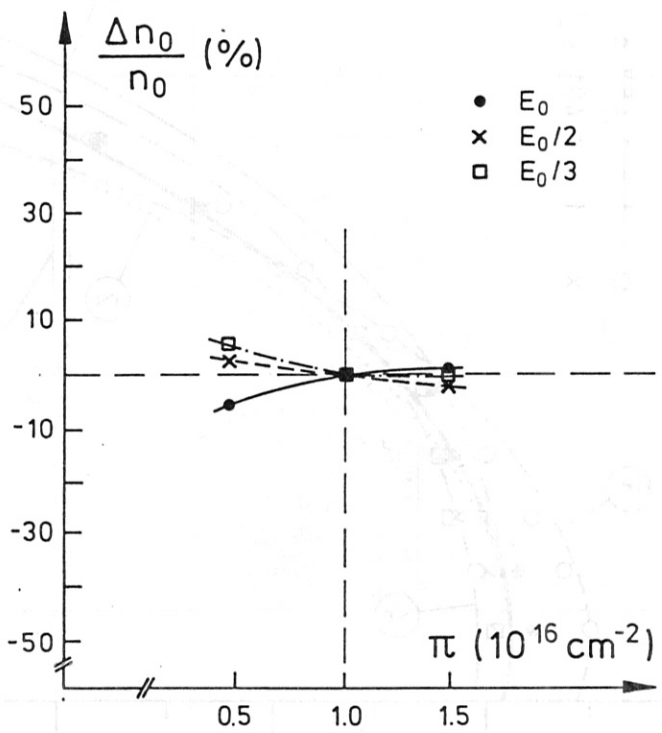


Fig. 7

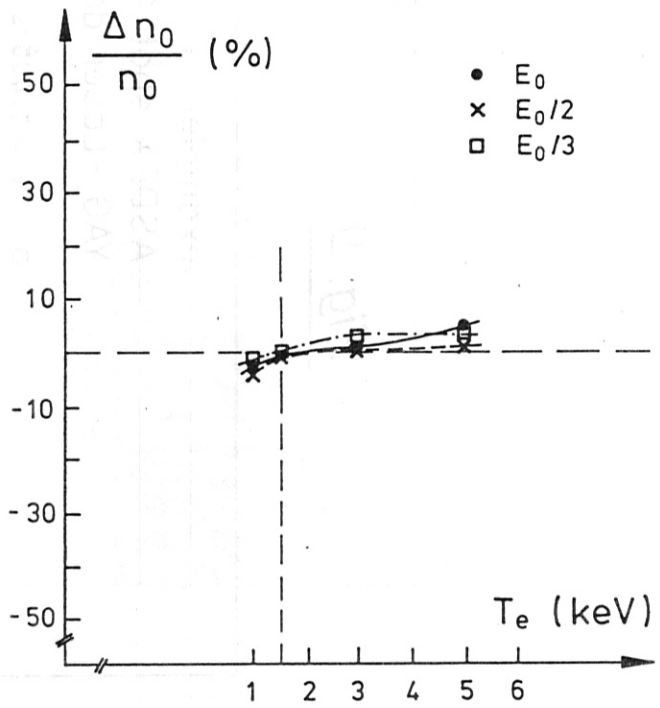


Fig. 8

# Fig. 9

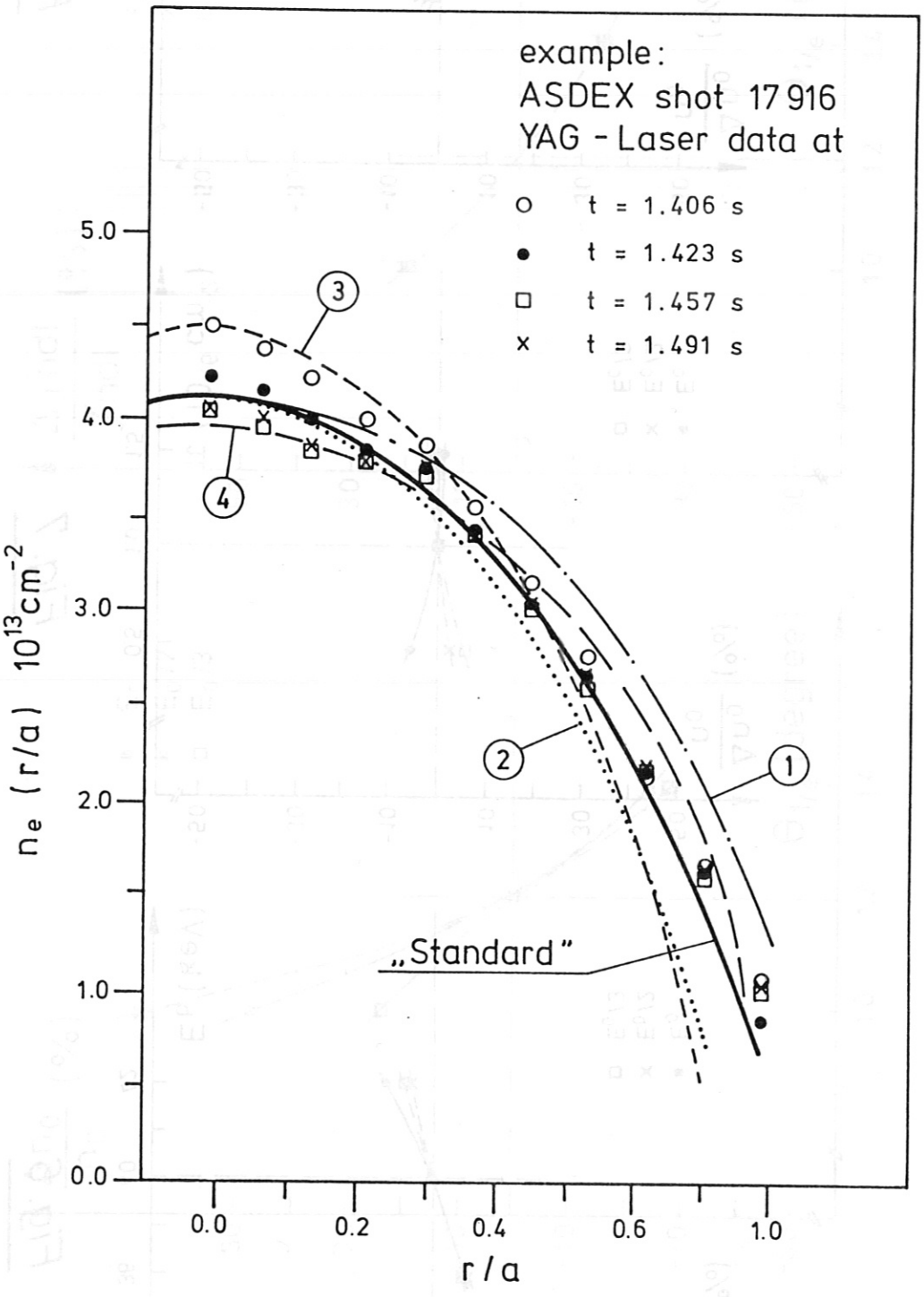
example:
ASDEX shot 17916
YAG - Laser data at
t = 1.406 s
t = 1.423 s
t = 1.457 s
t = 1.491 s
5.0
4.0
3.0
2.0
1.0
0.0
$n_e$ (r/a) $10^{13}cm^{-2}$
0.0
0.2
0.4
0.6
1.0
r / a
1
2
3
4
„Standard"

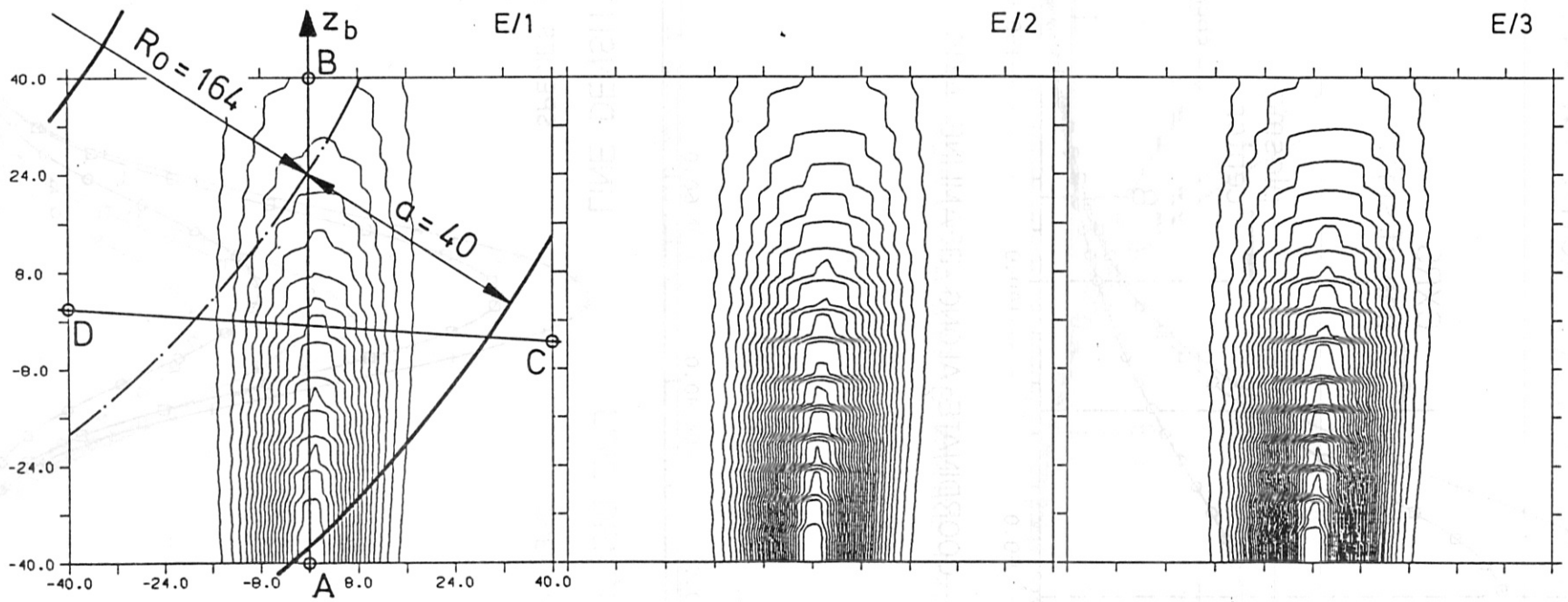
$z_b$
E/1
E/2
E/3
$R_0 = 164$
$a = 40$
B
D
C
A
40.0
24.0
8.0
-8.0
-24.0
-40.0
-40.0
-24.0
-8.0
8.0
24.0
40.0
a)
b)
c)

Fig. 10

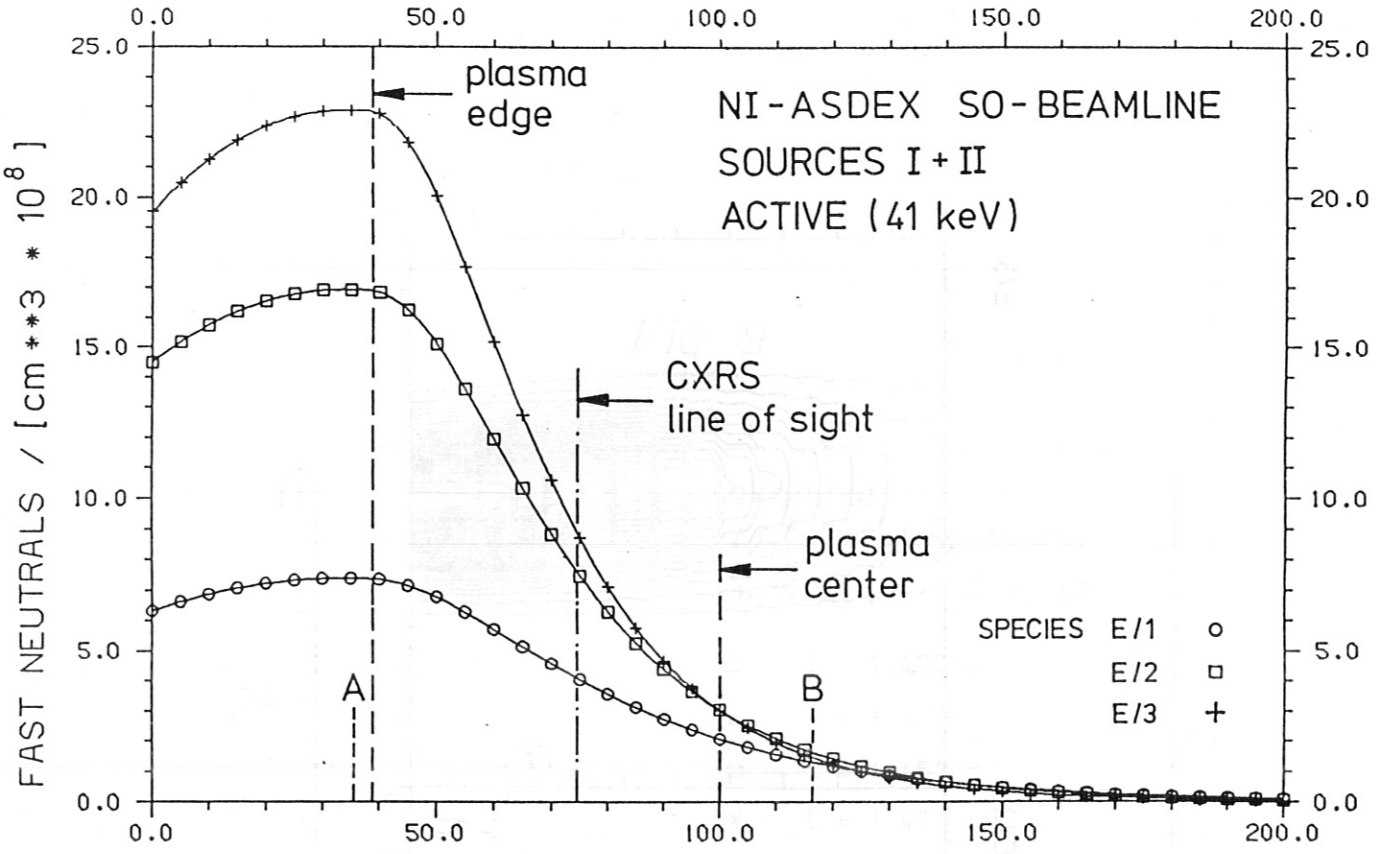


*Fig. 11a*

*Fig. 11b*

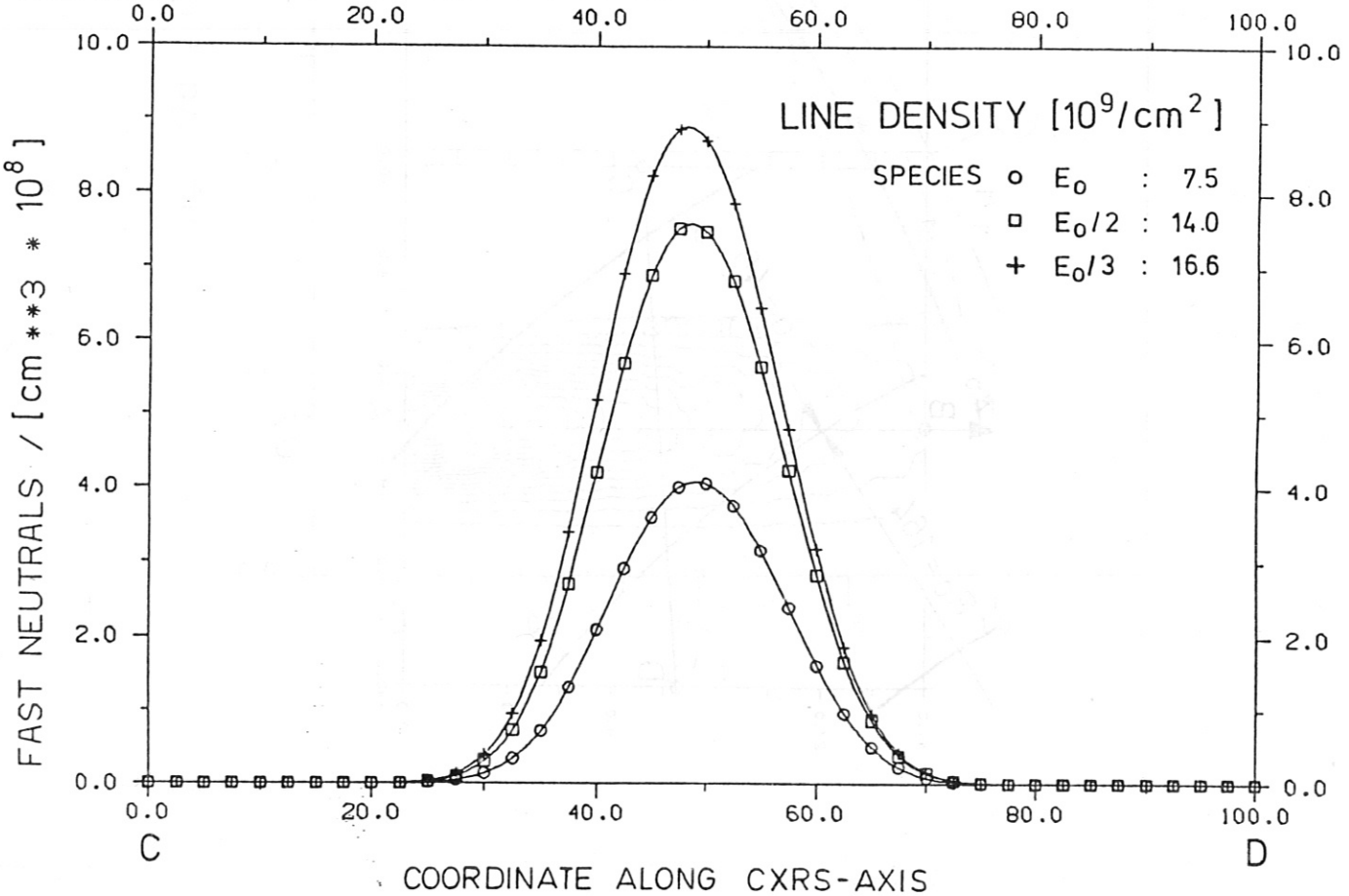

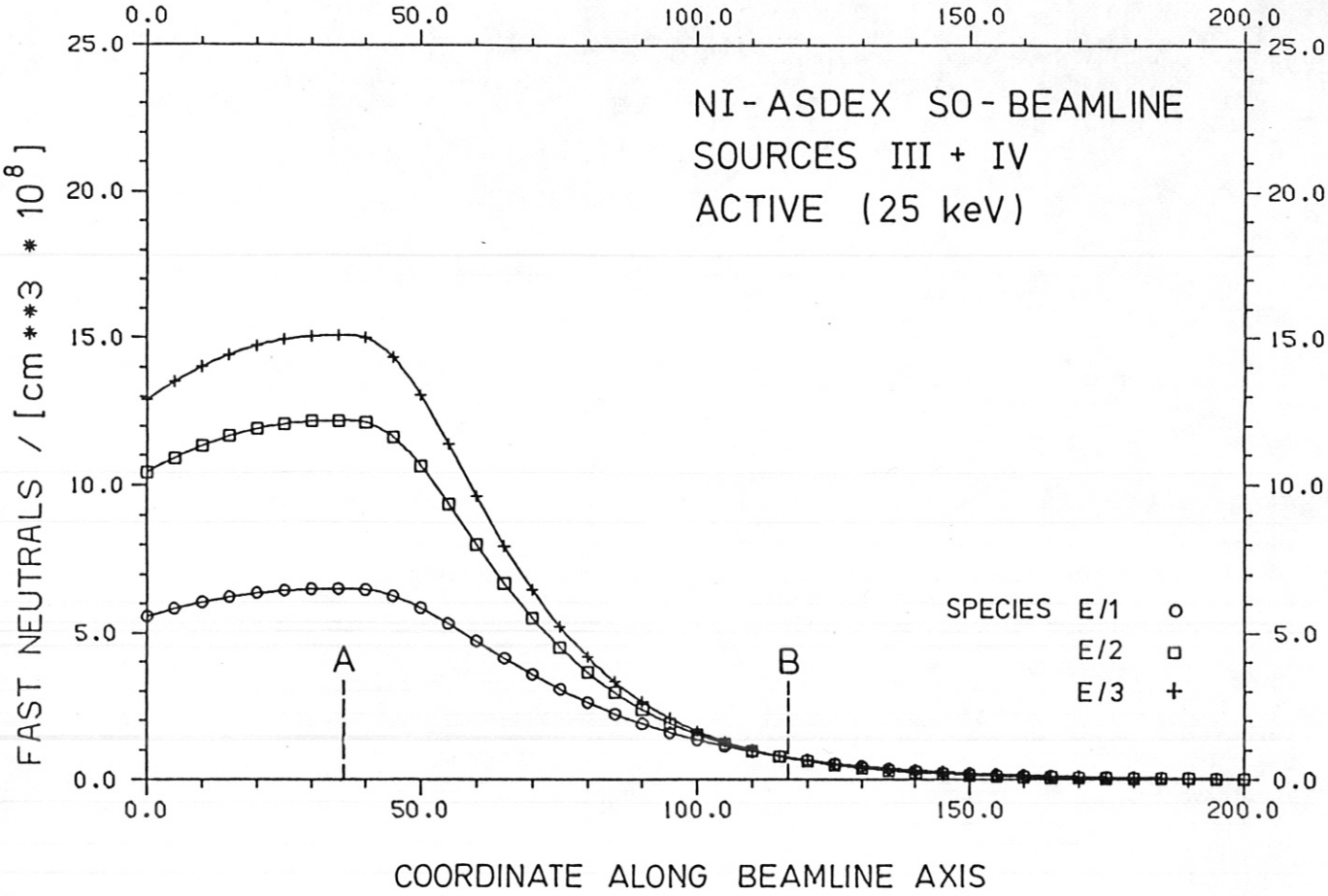


*Fig. 12 a*

*Fig. 12 b*